

# MODELLING OF ICRF HEATING AND CURRENT DRIVE IN TOKAMAK PLASMA WITH TWO ION SPECIES

*D.L. Grekov, S.V. Kasilov, K.K. Tretiak*

*Institute of Plasma Physics NSC “Kharkov Institute of Physics and Technology”, Kharkov, Ukraine*

*E-mail: grekov@ipp.kharkov.ua*

Fast magnetosonic wave propagation in real tokamak geometry is studied using a 2D finite difference code. Propagation and absorption of converted small scale waves is treated with help of the ray tracing code. Driven current densities are calculated in linear approximation using current drive efficiencies computed by the code SYNCH. It has been found that CD efficiency and current profile are almost independent of the toroidal antenna spectrum.

PACS: 52.70.-m

## INTRODUCTION

Ion cyclotron mode conversion regime (ICMC) is a popular regime for heating tokamak plasma with two ion species [1]. In most cases these species are hydrogen and deuterium. To understand the underlying physics of the heating, the model with one dimensional inhomogeneity of plasma parameters was exploited very often. At the same time, two dimensional effects play an essential role in propagation and absorption of both, launched fast magnetosonic wave (FMSW) and converted small scale wave. Depending on device and plasma parameters, the converted wave may be the ion Bernstein wave (IBW) or Alfvén wave (Stix mode, SW).

## 1. PROPAGATION OF FMSW

For computations of FMSW electromagnetic field distribution in a tokamak, a numerical code FAW2 has been developed. FAW2 allows a treatment of general tokamak magnetic field configurations including the poloidal divertor and realistic wall geometry using directly the equilibrium field data from the EFIT code. FAW2 uses the cylindrical coordinate system  $(R, \varphi, Z)$ , where  $Z$ -axis is the main axis of the torus. Code solves the following Maxwell equations

$$\frac{i\omega}{c} \frac{\partial B_\phi}{\partial Z} + \frac{\omega^2}{c^2} (\varepsilon_1 - N_\phi^2) E_R - \frac{\omega^2}{c^2} \frac{i\varepsilon_2}{b_\phi} E_Z - \frac{il_\phi}{R^2} \frac{\partial}{\partial R} (RE_\phi) + \frac{b_R}{b_\phi} \left\{ \frac{\partial}{\partial R} \left( \frac{il_\phi}{R} E_R \right) + \frac{il_\phi}{R} \frac{\partial E_Z}{\partial Z} - \frac{\partial}{\partial R} \left[ \frac{1}{R} \frac{\partial}{\partial R} (RE_\phi) \right] \right\} - \left. \frac{\partial^2 E_\phi}{\partial Z^2} - \frac{\omega^2}{c^2} \varepsilon_1 E_\phi \right\} = 0, \quad (1)$$

$$-\frac{i\omega}{c} \frac{1}{R} \frac{\partial}{\partial R} (RB_\phi) + \frac{\omega^2}{c^2} \frac{i\varepsilon_2}{b_\phi} E_R + \frac{\omega^2}{c^2} (\varepsilon_1 - N_\phi^2) E_Z - \frac{il_\phi}{R} \frac{\partial E_\phi}{\partial R} + \frac{b_Z}{b_\phi} \left\{ \frac{\partial}{\partial R} \left( \frac{il_\phi}{R} E_R \right) + \frac{il_\phi}{R} \frac{\partial E_Z}{\partial Z} - \frac{\partial}{\partial R} \left[ \frac{\partial}{\partial R} (RE_\phi) \right] \right\} - \left. \frac{\partial^2 E_\phi}{\partial Z^2} - \frac{\omega^2}{c^2} \varepsilon_1 E_\phi \right\} = 0, \quad (2)$$

$$\frac{i\omega}{c} B_\phi - \frac{\partial E_R}{\partial Z} + \frac{\partial E_Z}{\partial R} = 0, \quad (3)$$

on the equidistant  $(R, Z)$  mesh. Here  $\omega$  is the wave frequency,  $c$  is the speed of light,  $\varepsilon_1 = \varepsilon_{11}$ ,  $\varepsilon_2 = -i\varepsilon_{12}$  are the components of the “hot” plasma dielectric permittivity tensor in absence of the finite Larmor radius effects,  $\vec{E}(\vec{r}), \vec{B}(\vec{r}) = \vec{E}(R, Z), \vec{B}(R, Z) \exp(i\omega t - il_\phi \varphi)$ ,  $b_R, b_\phi, b_Z$  are the components of the unit vector in the direction of the magnetic field.  $N_\phi = l_\phi c / R\omega$ . Using the fact that

$$E_{||} \approx 0 \text{ for the FMSW, } E_\phi = -\frac{b_R}{b_\phi} E_R - \frac{b_Z}{b_\phi} E_Z \text{ is}$$

postulated. In addition, an artificial collisional damping is introduced in the components of plasma dielectric tensor in the vicinity of the conversion layer to simulate the transformation of FMSW into small scale waves. This allows one to estimate the spatial distribution of the converted power in the minor cross-section of the torus. FAW2 has been applied for calculation of FMSW propagation in JET-like tokamak plasma with light (H)

minority ions and D majority ions. The plasma density and temperature profiles have been of the form  $n_\alpha, T_\alpha(\psi) = n_{\alpha 0}, T_{\alpha 0} \frac{\exp \xi - \exp(\xi \psi)}{\exp \xi - 1}$  inside the separatrix, where  $\alpha = e, H, D$ ,  $\xi$  is the parameter ( $\xi = -5$  for density and  $\xi = 3$  for temperature profiles) and  $\psi$  is the flux surface label ( $\psi = 0$  at the plasma centre and  $\psi = 1$  at the separatrix). The following set of parameters has been used,  $B_0 = 18 \text{ kG}$ ,  $n_{e0} = 3.1 \cdot 10^{13} \text{ cm}^{-3}$ ,  $n_H/n_e = 0.14$ ,  $T_{e0} = 3 \text{ keV}$ . We have varied wave frequency from 27 to 31 MHz in order to change the position of conversion layer along the big radius of the torus  $R$ .

An example of wave field pattern in the minor cross-section of the torus is shown in Fig. 1. The focusing of the wave field to the region of plasma with highest

density is the dominant effect of 2D plasma inhomogeneity.

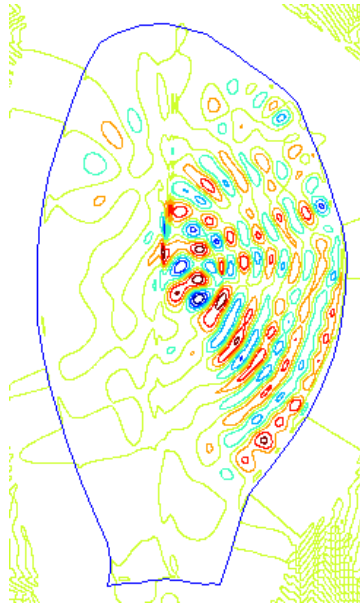


Fig. 1. Distribution of wave field  $B_\phi$  in the minor cross-section of the torus for toroidal wave number  $l_\phi = 18$

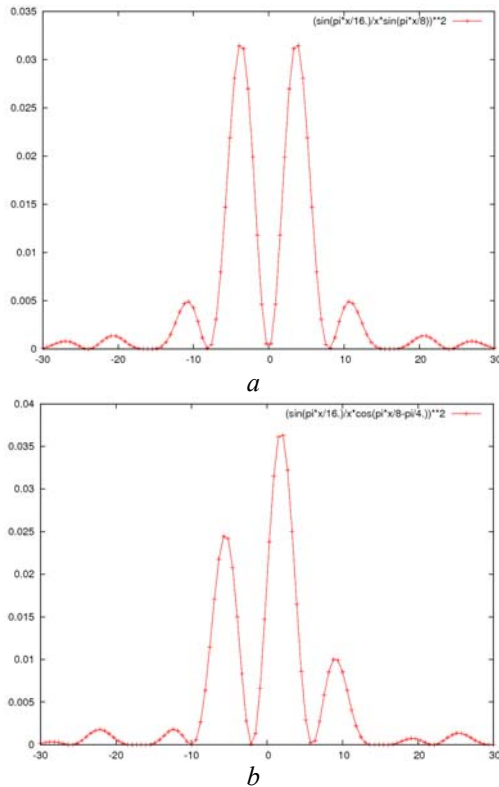


Fig. 2. Symmetric toroidal antenna spectrum (a). Asymmetric toroidal antenna spectrum (b)

Two types of antenna spectrum in toroidal direction have been used in the calculations as shown in Fig. 2. The number of toroidal harmonics taken into account has been limited to  $(|l_\phi| \leq 10)$  because higher harmonics give a negligible contribution to the total absorbed power. Practically all absorbed FMSW power is localized in the vicinity of the conversion zone which is a region highly localized over  $R$  variable around the

line  $R = R_c$ . In the reality, this power is transformed from the FMSW to small scale waves - the ion Bernstein wave (IBW) or Alfvén wave (Stix mode).

## 2. ICW AND SW PROPAGATION

Propagation and damping of small scale waves has been studied with the help of the ray tracing code which uses the same equilibrium parameters as FAW2. In contrast to FAW2, finite Larmor radius effects have been taken into account in this code. Code solves the equations

$$\begin{aligned} \frac{d\vec{r}}{dt} &= \frac{\partial D}{\partial \vec{k}} \bigg/ \frac{\partial D}{\partial \omega}, \\ \frac{d\vec{k}}{dt} &= - \frac{\partial D}{\partial \vec{r}} \bigg/ \frac{\partial D}{\partial \omega}, \end{aligned} \quad (4)$$

where  $\vec{k}$  is the wave vector and  $D(\omega, \vec{r}, \vec{k}) = 0$  is the following dispersion equation,

$$\begin{aligned} \eta N_\perp^6 + \eta N_\perp^4 (N_\parallel^2 - 2\varepsilon_1 - \varepsilon_3) + \varepsilon_1 N_\perp^4 + \eta N_\perp^2 2\varepsilon_3 (\varepsilon_1 - N_\parallel^2) + \\ N_\perp^2 [(\varepsilon_1 + \varepsilon_3)(N_\parallel^2 - \varepsilon_1) + \varepsilon_2^2] + \varepsilon_3 [(N_\parallel^2 - \varepsilon_1)^2 - \varepsilon_2^2] = 0. \end{aligned} \quad (5)$$

Here  $\vec{N} = \vec{k}c/\omega$ ,  $N_\parallel = \vec{N} \cdot \vec{B}/|\vec{B}|$ ,  $N_\perp^2 = N^2 - N_\parallel^2$  and

$$\eta = - \sum_i \frac{3\omega_{pi}^2 \omega^2 v_{Ti}^2}{c^2 (\omega^2 - \omega_{Bi}^2)(\omega^2 - 4\omega_{Bi}^2)}, \quad i = H, D.$$

Power carried by the ray  $Q$  is defined as  $Q = Q_0 e^{-\Gamma}$ ,

$$\Gamma = \int_0^t \text{Im} \vec{k} \frac{\partial \vec{r}}{\partial \tau} d\tau, \quad \text{where } Q_0 \text{ is the initial power at the ray}$$

starting point. Rays are started from the centers of equidistant intervals on the line  $R = R_c$  (conversion zone position). Typically 200 intervals over  $Z$  variable within the region limited by the separatrix have been used. Initial ray power values have been set to the integrals of the absorbed FMSW power density computed by FAW2 over the plasma volume limited by the respective  $Z$  interval.

For computation of radial profiles plasma volume within the separatrix has been divided into  $n$  zones limited by the equidistant  $\psi$  levels (typically  $n=40$ ). The absorbed powers and driven currents within each zone have been summed up over all the rays. In this way the dependencies of current drive efficiency and absorbed power on the flux surface label  $\psi$  have been obtained. Electron and minority ion current densities for the rays have been calculated in linear approximation using current drive efficiencies computed by the 2D kinetic equation solver SYNCH [2].

The numerous ray traces are shown in Fig. 3. FMSW rays are started at the high field side towards the low field side. As seen from in Fig. 3, FMSW rays started at the central part of the cross-section (near the mid-plane) are converted into IBW rays which propagate then back to the high field side. This is due to the smallness of the  $B_R$  component value of the equilibrium magnetic field there.

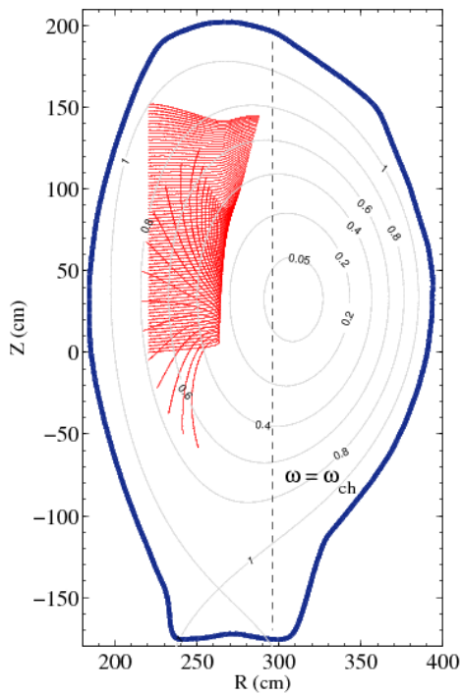


Fig. 3. Ray traces of FMSW, IBW and SW. Standard set of plasma parameters. Levels of  $\psi$  are shown with black lines labeled by  $\psi$  value

In turn, FMWS rays started at the upper part of the cross-section (further away from the mid-plane) are converted into SW and penetrated further to the cyclotron resonance zone of the minority ions.

The spatial distributions of the total current drive efficiency (summed up over the toroidal harmonics) are shown in Fig. 4 for the symmetric and asymmetric antenna spectra.

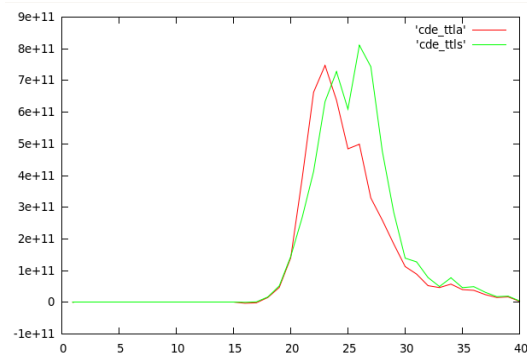


Fig. 4. Current drive efficiencies (a.u.) vs. magnetic surface index (0 – magnetic axis, 40 – separatrix). Red – asymmetric spectrum, green – symmetric spectrum

As seen from Fig. 4, there is no principal difference in CD efficiency between different ways of the FMSW excitation.

## CONCLUSIONS

While the separate toroidal harmonics of the launched FMSW spectrum demonstrate clear difference in propagation, absorption and CD efficiency in the mode conversion regime, total CD efficiency value and current density profile are almost independent of the antenna phasing in the toroidal direction

## REFERENCES

1. M.J. Mantinen et al. Application of ICRF waves in tokamaks beyond heating // *Plasma Physics and Controlled Fusion*. 2003, v. 45, p. A445-A456.
2. S.V. Kasilov, W. Kernbichler. Passive cyclotron current drive efficiency for relativistic toroidal plasmas // *Phys. Plasmas*. 1996, v. 3, №11, p. 4115-412.

Article received 24.01.13

## МОДЕЛИРОВАНИЕ НАГРЕВА И СОЗДАНИЯ ТОКОВ УВЛЕЧЕНИЯ В ОБЛАСТИ ИОННЫХ ЦИКЛОТРОННЫХ ЧАСТОТ В ТОКАМАКАХ В ПЛАЗМЕ С ДВУМЯ СОРТАМИ ИОНОВ

Д.Л. Греков, С.В. Касилов, К.К. Третьяк

Исследовано распространение быстрых магнитозвуковых волн в токамаке с учетом реальной геометрии установок при помощи двумерного конечно-разностного кода. Распространение и поглощение конвертированных мелкомасштабных волн изучалось методом лучевых траекторий. В линейном приближении рассчитаны плотности токов увлечения с использованием эффективности создания токов увлечения, вычисляемой кодом SYNCH. Показано, что эффективность создания и распределение тока увлечения почти не зависят от тороидального спектра антенны.

## МОДЕЛЮВАННЯ НАГРІВАННЯ І СТВОРЕННЯ СТРУМІВ ЗАХОПЛЕННЯ В ОБЛАСТІ ІОННИХ ЦИКЛОТРОННИХ ЧАСТОТ У ТОКАМАКАХ У ПЛАЗМІ З ДВОМА СОРТАМИ ІОНІВ

Д.Л. Греков, С.В. Касілов, К.К. Трет'як

Досліджено поширення швидких магнітозвукових хвиль у токамаках з урахуванням реальної геометрії установок за допомогою двовимірного скінченно-різницевого коду. Поширення та поглинання конвертованих дрібномасштабних хвиль було вивчено методом променевих траєкторій. У лінійному наближенні розраховано щільності стаціонарного струму захоплення з використанням ефективності утворення стаціонарного струму захоплення, що обчислювалась кодом SYNCH. Показано, що ефективність утворення та розподіл стаціонарного струму захоплення майже не залежать від тороїдального спектра антени.